The p53 Tumor Suppressor Network Is a Key Responder to Microenvironmental Components of Chronic Inflammatory Stress

Frank Staib,[1] Ana I. Robles,[1] Lyuba Varticovski,[1] Xin W. Wang,[1] Barry R. Zeeberg,[2] Michail Sirotin,[3] Victor B. Zhurkin,[3] Lorne J. Hofseth,[4] S. Perwez Hussain,[1] John N. Weinstein,[2] Peter R. Galle,[5] and Curtis C. Harris[1]

[1]Laboratories of Human Carcinogenesis, [2]Molecular Pharmacology, and [3]Experimental and Computational Biology, Center for Cancer Research, National Cancer Institute, NIH, Bethesda, Maryland; [4]Department of Basic Pharmaceutical Sciences, College of Pharmacy, University of South Carolina, Columbia, South Carolina; and [5]First Department of Internal Medicine, Johannes Gutenberg University of Mainz, Mainz, Germany

Abstract

Activation of the p53 network plays a central role in the inflammatory stress response associated with ulcerative colitis and may modulate cancer risk in patients afflicted with this chronic disease. Here, we describe the gene expression profiles associated with four microenvironmental components of the inflammatory response ($NO^{\bullet}$, H_2O_2, DNA replication arrest, and hypoxia) that result in p53 stabilization and activation. Isogenic HCT116 and HCT116 *TP53*$^{-/-}$ colon cancer cells were exposed to the $NO^{\bullet}$ donor Sper/NO, H_2O_2, hypoxia, or hydroxyurea, and their mRNA was analyzed using oligonucleotide microarrays. Overall, 1,396 genes changed in a p53-dependent manner ($P < 0.001$), with the majority representing a "unique" profile for each condition. Only 14 genes were common to all four conditions. Included were eight known p53 target genes. Hierarchical sample clustering distinguished early (1 and 4 hours) from late responses (8, 12, and 24 hours), and each treatment was differentiated from the others. Overall, $NO^{\bullet}$ and hypoxia stimulated similar transcriptional responses. Gene ontology analysis revealed cell cycle as a key feature of stress responses and confirmed the similarity between $NO^{\bullet}$ and hypoxia. Cell cycle profiles analyzed by flow cytometry showed that $NO^{\bullet}$ and hypoxia induced quiescent S-phase and G_2-M arrest. Using a novel bioinformatic algorithm, we identified several putative p53-responsive elements among the genes induced in a p53-dependent manner, including four [*KIAA0247, FLJ12484, p53CSV* (*HSPC132*), and *CNK* (*PLK3*)] common to all exposures. In summary, the inflammatory stress response is a complex, integrated biological network in which p53 is a key molecular node regulating gene expression. (Cancer Res 2005; 65(22): 10255-64)

Introduction

Inflammatory responses caused by infectious and noninfectious external factors induce reactive oxygen and nitrogen species. Included are hydrogen peroxide (H_2O_2), nitric oxide ($NO^{\bullet}$), and reactive intermediates such as hydroxyl radicals ($OH^{\bullet}$), superoxide ($O_2^{-\bullet}$), and peroxynitrite ($ONOO^-$). To reduce the level of reactive oxidants and limit their damaging effects (particularly to DNA, RNA, proteins, and lipids), several defense mechanisms have evolved. One of the genes at the crossroads of cellular stress response networks is *p53*, a prominent tumor suppressor (reviewed in refs. 1, 2). Chronic infections and chronic inflammatory diseases, such as ulcerative colitis, result in a prolonged oxidative and nitrosive stress and an increased cancer risk (reviewed in ref. 2). Recently, we described the role of p53 activation in $NO^{\bullet}$-induced cellular stress (3) and chronic inflammation (4). We have also reported a positive correlation between elevated levels of the inducible nitric oxide synthase (iNOS) and increased *TP53* mutation load in chronically inflamed colon tissue from patients with ulcerative colitis (5) and other chronic inflammatory diseases (6). We, therefore, hypothesized that the inflammatory microenvironment both activates the p53 network and inactivates the tumor suppressor activity by mutation of the *p53* gene (7). *TP53* mutations contribute to clonal cellular expansion and genomic instability through deregulation of cell cycle checkpoints, DNA repair, and apoptosis (8, 9). Free radicals, as well as hydroxyurea, can also lead to DNA replication stress involving the ATR kinase network (10, 11).

In addition to reactive oxidants, the microenvironmental changes within inflamed tissues are typically associated with hypoxic conditions, in which oxygen tensions <10 mm Hg (i.e., <1% oxygen) have been reported (12). Thus, hypoxia is an additional cell stress mediator concurrently found during chronic inflammation. Hypoxia leads to stabilization of the transcription factor HIF-1α and induces p53 accumulation and activation through the ATR kinase (13). Thus, p53's protective functions are also required to control the cellular response to hypoxia, and cells with mutated *TP53* may have a growth advantage (reviewed in refs. 2, 14). Beyond the cellular stress caused by reduced oxygen, lactate and metabolic acidosis accumulate, contributing to cellular stress (15). Thus, cellular stress is a multifaceted condition generated by free radical species, hypoxia, and other factors that target the nuclear factor-κB (NF-κB) and other stress response networks (16).

Microarray-based gene expression analysis offers the opportunity to profile the gene expression changes in cells exposed to stress. In the present study, we exposed HCT116 and its isogenic HCT116 *TP53*$^{-/-}$ colon cancer cell line to the $NO^{\bullet}$ donor Sper/NO, H_2O_2, hypoxia, or hydroxyurea and assessed gene expression. That study design enabled us to compare the gene expression response of isogenic cells differing in *TP53* status with four different stress

Note: Supplementary data for this article are available at Cancer Research Online (http://cancerres.aacrjournals.org/).

The original data will be available at the National Center for Biotechnology Information's Gene Expression Omnibus public database (http://www.ncbi.nlm.nih.gov/geo) as GSE 3176 at a later date.

Requests for reprints: Curtis C. Harris, Laboratory of Human Carcinogenesis, National Cancer Institute, NIH, 37 Convent Drive, Room 3068, MSC 4255, Bethesda, MD 20892-4255. Phone: 301-496-2048; Fax: 301-496-0497; E-mail: Curtis_Harris@nih.gov.

doi:10.1158/0008-5472.CAN-05-1714

conditions frequently found during chronic inflammation. Those stress conditions have at least one factor in common: activation of the p53 network. The transcriptional effects of that activation were addressed by two different analytic approaches. In the first, we analyzed gene expression during the stress response in HCT116 cells, which have functional p53 networks. In the second approach, we analyzed differences in gene expression between the two nominally isogenic genotypes, resulting in the identification of known and novel p53 transcriptional targets.

Materials and Methods

Cell culture and exposures. HCT116 and HCT116 *TP53*$^{-/-}$ colon cancer cell lines, a kind gift from Bert Vogelstein (Johns Hopkins School of Medicine, Baltimore, MD), were maintained in McCoy's 5A medium containing 10% fetal bovine serum, 4 mmol/L glutamine, 10 units/mL penicillin, and 10 μg/mL streptomycin (Biofluids, Rockville, MD). Cells were seeded at $\sim 7 \times 10^4$/mL, grown to 70% confluence, and exposed to freshly prepared 1 mmol/L Sper/NO (Alexis Biochemicals, San Diego, CA), 0.1 mmol/L H_2O_2, 1.5 mmol/L hydroxyurea or hypoxia (Anaerocult A-mini, EMD Chemicals, Gibbstown, NJ). The Anaerocult A-mini system generates O_2 concentrations <0.5% and CO_2 concentrations >10% within 60 minutes. O_2 concentrations <0.1% are reached after 160 minutes (17).[6] Hypoxic conditions were confirmed using indicator strips (Anaerotest, EMD Chemicals). Cells were harvested at the specified time points.

Whole cell lysate and Western blot analysis. Cells lysates (4) were separated by SDS-PAGE, transferred onto nitrocellulose, and analyzed using the following antibodies: monoclonal anti-human p53 (DO-1 clone, Calbiochem, San Diego, CA), polyclonal anti-human p53 phospho-Ser^{15} (Cell Signaling, Beverly, MA), and monoclonal anti-human actin (clone C4, Roche Diagnostics, Indianapolis, IN). The Western blot bands were quantified by densitometry using AIDA/2D Densitometry 2.0 software (Raytest, Wilmington, NC).

RNA isolation, microarray hybridization, data analysis, and validation by quantitative reverse transcription-PCR. Total RNA was isolated using Trizol reagent (Invitrogen, Carlsbad, CA) according to the manufacturer's instructions. A detailed description of the microarray hybridization, data analysis, and validation experiments is available in the Supplementary Notes.

Briefly, fluorescence-labeled cDNA (Cy3 and Cy5) was generated using 20 μg total RNA. Cy3-labeled reference probes (0-hour time points) and Cy5-labeled probes (samples exposed for the indicated times) were hybridized to 70-mer oligonucleotide microarrays with 21,329 probes (Qiagen Human Array-Ready Oligo Set, version 2.0). The arrays were printed by the Advanced Technology Center at the National Cancer Institute. At least two hybridizations (range, 2-5) were done for each sample. We used the following software for data analysis: BRB Array Tools developed by Dr. Richard Simon and Amy Peng Lam (http://linus.nci.nih.gov/BRB-ArrayTools.html), High-Throughput GoMiner (18), and PathwayAssist (Iobion Informatics, LLC, La Jolla, CA). To identify putative p53-responsive elements in selected candidate genes, we used a newly constructed position weight matrix.[7]

For data validation by quantitative reverse transcription-PCR (RT-PCR), 10-μg samples of total RNA, isolated from independent exposure experiments, were reverse-transcribed using the High-Capacity cDNA Archive Kit. The amplification was done using Taqman Universal PCR Master Mix and predeveloped 6-FAM dye-labeled Taqman assays (Assays-on-Demand, Applied Biosystems, Foster City, CA) for the following genes: *SNK* (*PLK2*), *CDKN1C, POLE2, CPE, CNK* (*PLK3*), *PMAIP1, RAI3*, and *DDB2*. VIC dye-labeled human β-actin was used as external control.

Flow cytometry. Cells were labeled with 10 μmol/L bromodeoxyuridine (BrdUrd, BrdU) during the last 30 minutes of a 24-hour exposure. Staining with FITC-conjugated anti-BrdUrd antibody (BD Biosciences, San Jose, CA) and propidium iodide (Sigma-Aldrich, St. Louis, MO) was done as previously described (4). No less than 10,000 cells were analyzed by bivariate flow cytometry, using FACSCalibur and Cell Quest Pro software (BD Biosciences).

Results

p53 accumulation and activation in response to various cellular stresses. To determine the overall and p53-dependent transcriptional responses to different types of inflammatory stress, we exposed the *TP53*^{wt} and *TP53*$^{-/-}$ HCT116 colon cancer cell lines to NO•, H_2O_2, hydroxyurea, or hypoxia in time course experiments for up to 24 hours. The conditions for each exposure were chosen for comparable activation of the p53 network using p53 protein accumulation and posttranslational modification as surrogate indicators.

The Western blots shown in Fig. 1 all display similar p53 accumulation, although with different kinetics, upon exposure to the various stress conditions. Maximal accumulation of p53 was observed after 4 hours of exposure to H_2O_2, 8 hours of exposure to NO•, or 12 hours of exposure to hydroxyurea or hypoxia. All stress conditions resulted in p53 phosphorylation with kinetics similar to those of p53 accumulation, indicating p53 activation. As expected, no p53 expression was observed in *TP53*$^{-/-}$ cells (Supplementary Fig. 1). NO• or H_2O_2 exposure resulted in a comparable degree of DNA damage by Comet Assay (Supplementary Fig. 2A and B). Based on those observations, we selected three time points, representing early, maximal intermediate, and late transcriptional response, for expression profiling. The first, 1-hour exposure, already showed p53 accumulation and/or phospho-Ser^{15} p53 for all stresses. The second represented the maximum of p53 protein accumulation, which occurred at 8 hours for NO•-treated cells, at 4 hours for H_2O_2, and at 12 hours for hydroxyurea- and hypoxia-treated cells. The third time point was 24 hours of exposure for all conditions. We did not observe any significant toxicity from any of the treatments over the 24-hour period of exposure.

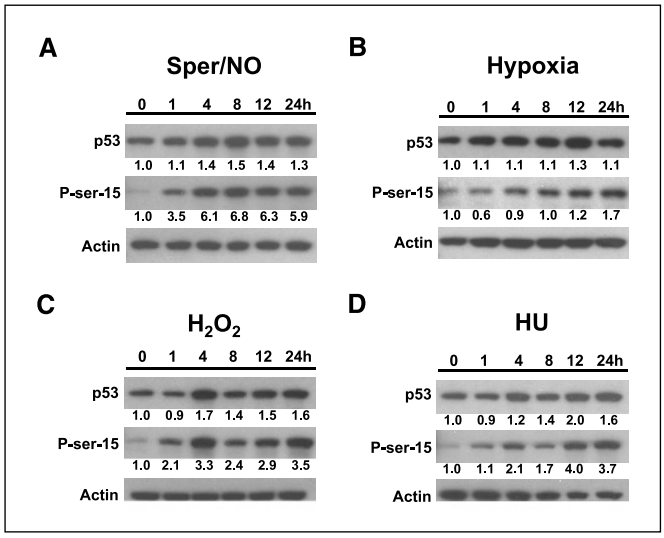

Figure 1. Western blot of p53 accumulation and posttranscriptional modification. HCT116 cells were exposed to (*A*) 1 mmol/L Sper/NO, (*B*) hypoxia, (*C*) 0.1 mmol/L H_2O_2, or (*D*) 1.5 mmol/L hydroxyurea (*HU*) for the indicated times (hours). Numbers below the blots indicate densitometry values as a ratio relative to the values of the untreated (0 hour) samples.

[6] A. Imhof, personal communication.
[7] M. Sirotin et al., in preparation.

Treatment-specific gene expression profiles. Genes significantly modulated by each exposure were identified by BRB Array Tools using class comparison analysis with univariate *F* test ($P < 0.001$) and a global permutation test ($P < 0.004$). For this analysis, each time variable was considered a class, and each exposure type was analyzed separately. There were 1,997 genes modulated by $NO^{\bullet}$, 838 genes by H_2O_2, 1,054 genes by hydroxyurea, and 1,652 genes by hypoxia. Figure 2*A* shows a dendrogram of hierarchical clustering of the samples based on the 4,047 genes identified by *F* tests as modulated by at least one of the exposure types. The hybridization replicates for each condition cluster together, indicating reproducibility of the data across arrays. The modulated genes clearly distinguish "early-response" and "late-response" samples (Fig. 2*A*). The early-response branch includes the 4-hour H_2O_2 and all 1-hour samples, subdivided into the four treatments. The late-response branch includes all 8-, 12-, and 24-hour exposures and discriminates hydroxyurea- or H_2O_2-treated cells from $NO^{\bullet}$- or hypoxia-treated cells. As an indicator of the robustness of the clustering, we computed the "*R*" measure after the dendrogram was cut into three clusters (Fig. 2*A, dashed horizontal line*). The *R* measure of 1.0 indicates that the clustering is highly robust and emphasizes that the pattern of gene modulation is unique to each exposure type. Of note, unbiased selection of 3,367 genes filtered for log ratio variation >0.01 and no more than 5% missing values across all experiments, resulted in similar discrimination of early versus late responses and overall similarity of response between hypoxia and $NO^{\bullet}$ as well as between hydroxyurea and H_2O_2 (Supplementary Fig. 3).

The "uniqueness" of each stress condition is also highlighted by the Venn diagram in Fig. 2*B*. The majority of the modulated genes changed their expression significantly in response to only one type of exposure. Only 40 genes of 4,047 total were significantly affected by all four treatments. Assuming total independence of the exposures, the expected value would be $(1{,}396/4{,}047)^4 \times 4{,}047 = 57.3$. The 40 genes are listed in Fig. 2*C* along with a hierarchical gene cluster analysis using individual array replicates. Most of them were up-regulated at 1 hour but changed to different degrees over time. Six genes in a small cluster were up-regulated at the intermediate and late time points, preferentially in response to hypoxia and $NO^{\bullet}$.

Nonoverlapping genes from each treatment shown on the Venn diagram in Fig. 2*B* are further categorized in Fig. 2*D* as up-regulated or down-regulated. About two thirds or 64% (1,270 of 1,997) of the genes modulated by $NO^{\bullet}$ were down-regulated. Similarly, 61% (648 of 1,054) of the genes were down-regulated by hydroxyurea and 54% (455 of 838) by H_2O_2. The gene expression profiles of cells exposed to hypoxia differed from those of the other three treatments; only 21% (343 of 1,652) were down-regulated.

Using PathwayAssist, we further analyzed the 40 genes whose change was common to all four exposures (Venn diagram, center, Fig. 2*B*). The analysis looked for the shortest paths connecting genes with each other or with different types of nodes (e.g., enzymes, cellular processes, or functional classes). The resulting Biological Association Network (BAN) is presented in Fig. 3. Early-response genes *JUN* and *FOS*, as well as p53, were incorporated into the BAN occupying central places. Cellular processes, such as apoptosis, death, and proliferation, were also identified and incorporated into the network (highlighted). So were the nodes for "hypoxic treatment" as well as the "HIF-1 complex." The 40 genes regulated in common by all stress conditions are associated with many of the cellular networks (including the p53 network) known to be involved in responses to severe stress.

To facilitate interpretation of the significant time course–related genes from the four exposures, as determined by *F* tests, we used High-Throughput GoMiner, a program that organizes genes of interest in the context of the Gene Ontology (19). That program enabled us to focus on groups of genes with similar functions or genes involved in the same network (18). A hierarchical clustering of the resulting Gene Ontology categories is depicted in Fig. 4. Several of the categories were affected only by $NO^{\bullet}$ and hypoxia (upper third of the category clusters). That observation supports the close relationship between $NO^{\bullet}$ and hypoxia detected in the previous analysis (Fig. 2*A*). Two clusters consisting of 16 Gene Ontology categories were affected by all four exposures. Interestingly, one-half of those are cell cycle–related categories. Included were G_1-S and G_2-M cell cycle checkpoints and M phase–specific microtubule processes. The category "DNA replication," identified in $NO^{\bullet}$ and hypoxia exposures, overlapped with the H_2O_2-related gene expression profile. The lower half of the hierarchical cluster contains Gene Ontology categories, affected only by $NO^{\bullet}$ or hypoxia. However, a subset of those categories, mainly "DNA replication initiation," "Protein metabolism," and "Macromolecule metabolism," was shared by H_2O_2 exposure and hypoxia.

Cell cycle analysis by flow cytometry (fluorescence-activated cell sorting). Gene Ontology analysis indicated that cell cycle regulation was a prominent feature for all exposures. Therefore, we analyzed cell cycle and DNA synthesis profiles in $TP53^{wt}$ and $TP53^{-/-}$ cells at the end of each exposure (Fig. 5*A* and *B*). As expected, hydroxyurea resulted in S-phase arrest, with >65% BrdUrd incorporation in $TP53^{wt}$ and $TP53^{-/-}$ cells compared with ~35% in the respective untreated cells. In contrast, H_2O_2 led to G_2-M arrest, more pronounced in the $TP53^{-/-}$ cells than in the $TP53^{wt}$ ones. That pattern is typical for DNA-damaging agents. The preferential bypass of G_1 arrest and increase in G_2-M arrest observed is also typical for DNA damage response in p53-deficient cells. Very significant changes in the cell cycle profile were observed after $NO^{\bullet}$ exposure as well. There was a pronounced decrease in BrdUrd incorporation in cells with S-phase DNA content, a condition previously described as quiescent S phase (4, 15), along with a significant arrest in G_2-M. The effect of hypoxia was similar to that of $NO^{\bullet}$, with a complete loss of active (BrdUrd positive) S-phase and G_2-M arrest.

p53-dependent gene expression profiles. To examine further the contribution of p53 activation to gene expression following different types of cellular stress, we did pairwise comparisons between gene expression in HCT116 and HCT116 $TP53^{-/-}$ cells for each time point and each treatment, using the univariate two-sample *t* test ($P < 0.001$) with randomized variance. A total of 842 genes, of which 399 were induced, were differentially expressed in a p53-dependent way upon $NO^{\bullet}$ exposure. The other three treatments resulted in fewer genes differentially expressed in a p53-dependent way. Exposure to H_2O_2 resulted in the differential expression of 272 genes, of which 187 were induced. Exposure to hydroxyurea resulted in the differential expression of 283 genes, of which 184 were induced, and exposure to hypoxia resulted in the differential expression of 315 genes, of which 177 were induced. Altogether, a total of 1,396 single genes were affected in a p53-dependent way by at least one of the four exposures, and 746 of them were induced. The 746 up-regulated genes contained 28 of a list of 53 previously reported p53 transcriptional target genes (Supplementary Table 1). That constituted a 15-fold enrichment

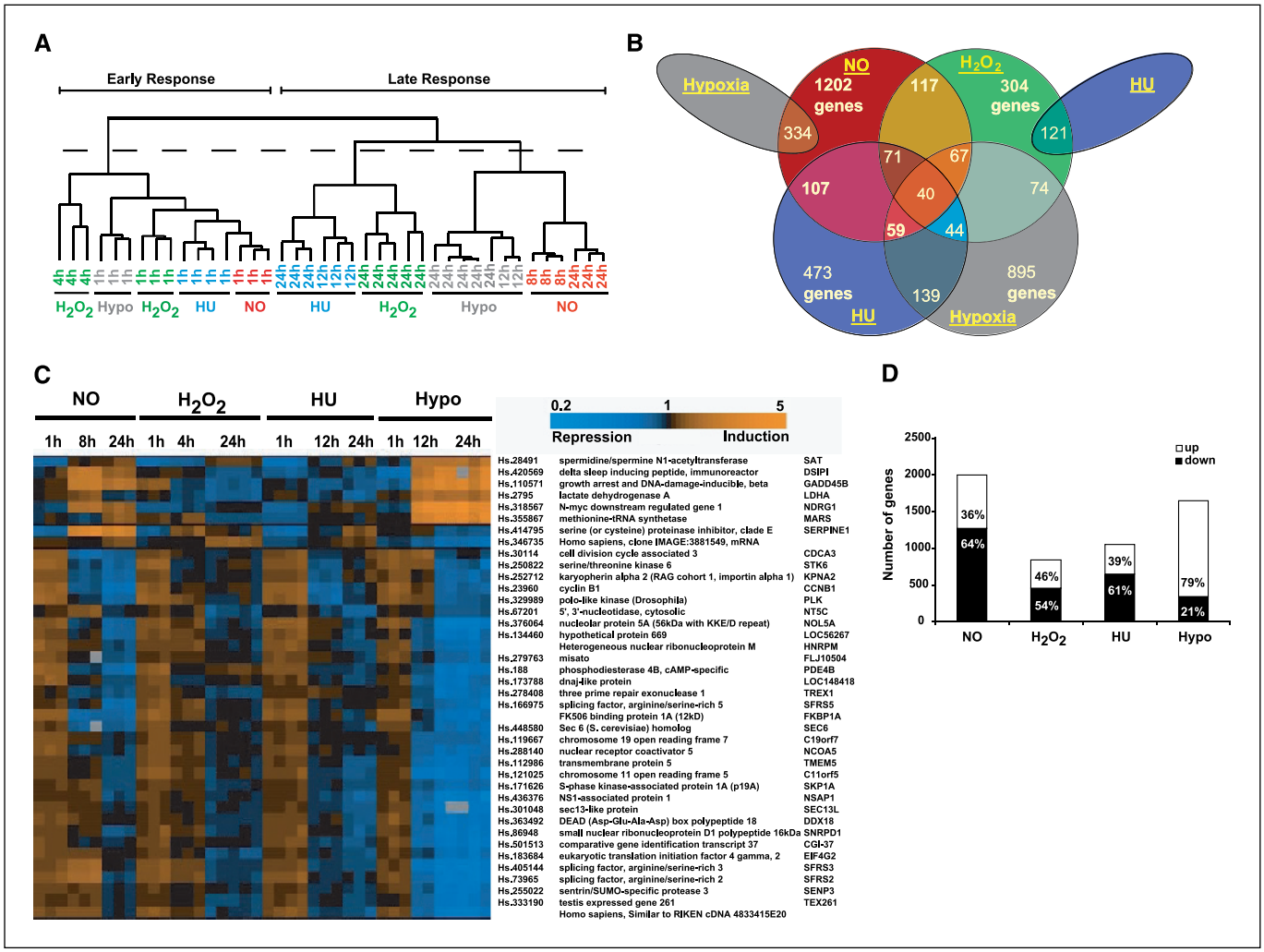

Figure 2. Time course of treatment-specific gene expression profiles as determined by univariate *F* test ($P < 0.001$) and controlled by a global permutation test. *A,* hierarchical clustering of samples based on the compiled list of 4,047 genes identified by BRB Array Tools as changing significantly over the time course under any exposure in HCT116 *TP53*^{wt}. For calculation of the robustness index, the cluster was cut into three trees as indicated by the black-dashed horizontal line (*R* index = 1.0 for each tree). *B,* Venn diagram depicting the number of overlapping or treatment-specific genes identified by *F* test as changing significantly over the time course for each exposure. There are 40 genes whose expression overlaps with all four exposures. *C,* hierarchical clustering of the 40 genes from the center of the Venn diagram, using all *TP53*^{wt} hybridization replicates for each time point and treatment. Unigene number, gene name, and description (*right*). Color-coded degree of expression (0.2- to 5-fold) relative to the untreated samples (*top right*). *D,* the total number of significant differentially expressed, nonoverlapping genes of each treatment (*F* test) is divided into up-regulated (*white columns*) and down-regulated (*black columns*) genes.

over random chance. The highest frequency of known p53 target genes (19 of 187, 10.2%) was observed in response to H_2O_2. There was specificity within the p53 transcriptional response in that some of the known p53 target genes were induced by only one treatment. For example, *GADD45A* and *TP53I11* (*PIG11*) were induced by NO$^{\bullet}$; *GPX1* was induced by H_2O_2; *APAF1* was induced by hydroxyurea; and *IGFBP3* was induced by hypoxia.

To assess the overall contribution of p53 activation, we used the set of 1,396 genes found to be p53 dependent in at least one of the individual *t* tests to generate a sample cluster tree (Supplementary Fig. 4), based on the array replicates, time points, and stress conditions (as in Fig. 2*A*). The resulting cluster tree showed remarkable similarities to the dendrogram consisting of genes that changed significantly over the time course (*F* test, Fig. 2*A*). Hybridization replicates of each condition clustered together. The arrays that defined "early" and "late" responses in Fig. 2*A* were similarly grouped, and there were consistent modulations of gene expression over time across the different types of exposure. The relationships between NO$^{\bullet}$ and hypoxia and between hydroxyurea and H_2O_2 seen in Fig. 2*A* were also preserved. Hierarchical clustering of samples from the intermediate time points based on the same 1,396 p53-dependent genes yielded the expected discrimination between *TP53*^{wt} and *TP53*$^{-/-}$ genotypes (data not shown).

As indicated in Fig. 2*A*, the temporal pattern of gene modulation was quite consistent, regardless of type of exposure. However, each exposure type was always clearly discriminated from the others, suggesting a degree of specificity in the p53-mediated transcriptional response. That specificity was further evidenced by the Venn diagram in Fig. 6*A*, which was generated using all 1,396 p53-dependent genes. Only a small fraction of genes were modulated in two, three, or all four p53-mediated gene expression profiles. This observation is consistent with Fig. 2*B*, in which genes modulated by all exposures, regardless of p53 dependence, were similarly grouped.

The 14 genes in the center of the Venn diagram in Fig. 6*A* are listed in Fig. 6*B* together with a dendrogram generated using the array replicates corresponding to the maximum p53 accumulation by Western blot (Fig. 1). The majority of genes in the group are p53 target genes and showed varying degrees of p53-dependent up-regulation [*BTG2, DDB2, FDXR, p53CSV* (*HSPC132*), *PLAB, SESN1*, and *SNK* (*PLK2*)]. In addition, *DKK1*, another p53 target gene, was induced by NO•, H_2O_2, or hydroxyurea, but repressed by hypoxia at 24 hours (data not shown). The general consistency of those results suggests that the data set and *t* test analysis may be useful in the identification of new p53 target genes.

The total number of genes differentially expressed (induced or repressed) in a p53-dependent manner for each time point and exposure type is depicted in Fig. 6*C*. As expected, there was a trend toward an increasing number of genes with time of exposure. It was also clear from these diagrams that the kinetics of p53-mediated gene expression is specific to each exposure type. More than 80% of the genes differentially expressed by 1 hour of exposure to NO• were repressed, whereas almost 90% of the genes differentially expressed by 1 hour of exposure to hypoxia were induced. Those proportions were very similar to changes in gene expression found by the *F* test (Fig. 2*D*). They indicate that signal transduction pathways intersecting with p53 transcription are uniquely activated upon each type of stress exposure. The proportions of induced genes are maximal at the same time point that showed maximum accumulation of p53 protein by Western blot (Fig. 1).

The identity and fold expression change of the top 20 most up-regulated or down-regulated genes for each of the four stress conditions are shown in the Supplementary Table 2A-D. Greater expression changes were observed with NO• and hypoxia than

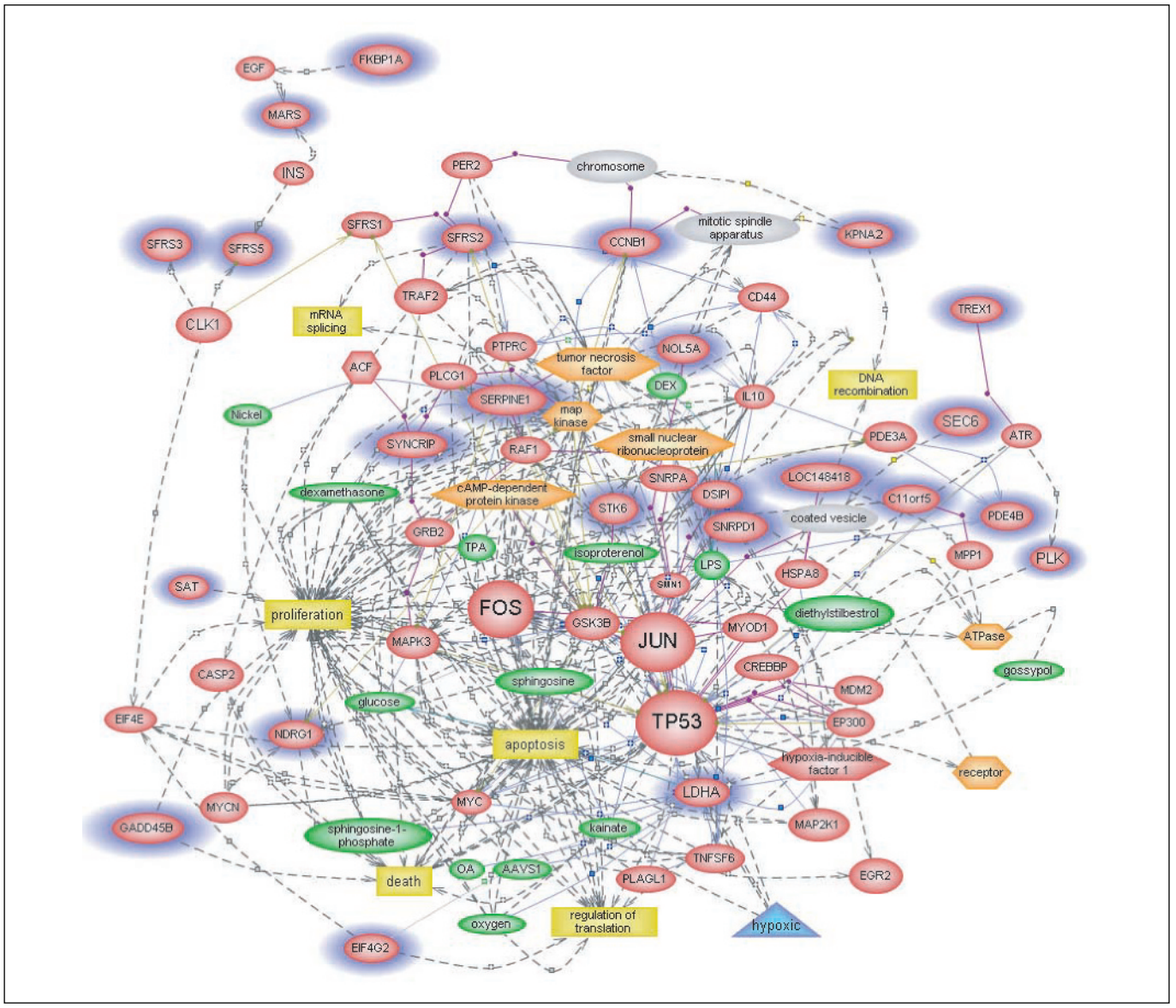

Figure 3. BAN using PathwayAssist for the 40 genes with gene expression changes common to all four exposures. The colors represent PathwayAssist categories: *red,* gene; *yellow,* cell process; *green,* small molecule; *orange,* protein functional class; *gray,* cell object; *blue,* treatment. Only genes (*blue halos*) that could be linked from the 40 selected genes to other genes, functions, or categories are included in the BAN. Among the genes introduced by PathwayAssist that link the genes of interest and/or their categories were *TP53* and the early-response genes, *JUN* and *FOS*. Cellular processes, such as "apoptosis," "death," and "proliferation," are also incorporated into the network, as were the nodes for "hypoxic treatment" and "HIF-1 complex."

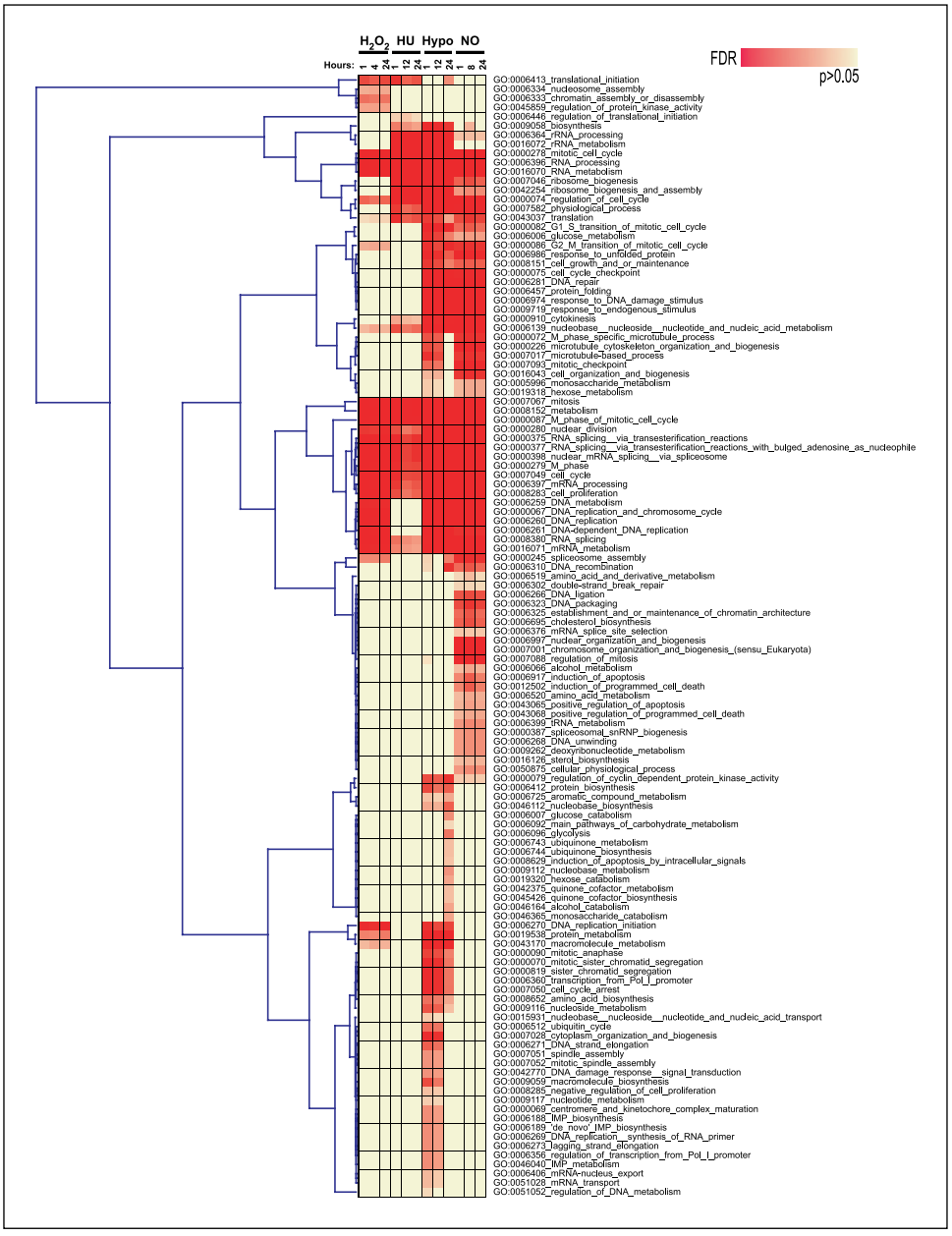

Figure 4. Functional categorization by High-Throughput GoMiner based on the Gene Ontology of the sum of 4,047 differentially expressed genes from Fig. 2*A*. These data were visualized by the publicly available software "Genesis" using the Pearson correlation and complete linkage clustering of the significant Gene Ontology categories. Categories with similar false discovery rate values tend to cluster together. False discovery rate is color coded (*top right*).

with hydroxyurea and H_2O_2. The top 20 gene lists included 12 previously described p53 target genes for hydroxyurea, nine for NO•, six for H_2O_2, and one for hypoxia.

Novel candidate p53 target genes. Well-characterized p53-responsive genes usually contain p53-binding sites within either their promoter or their first intron sequences. The p53-responsive element (p53RE) has been defined as two decamers of the palindromic consensus sequence RRRCWWGYYY (where R is a purine, W is adenine or thymine, and Y is a pyrimidine) separated by a 0- to 13-bp spacer. Because of the degeneracy of this sequence, it has been difficult to reliably identify p53RE in the regulatory regions of genes solely based on adherence to the consensus sequence. A novel approach uses the so-called position weight matrix (PWM) method (20). We have developed an algorithm based on a PWM generated by combining 34 experimentally validated p53RE (Supplementary Table 1) from genes known to be transcriptional targets of p53. That PWM was applied to all genes in the center of the Venn diagram in Fig. 6*A* (genes modulated in a p53-dependent manner by all four stresses). All previously validated p53REs within that set of genes were found by the PWM algorithm. Most interestingly, novel putative p53REs were found in the predicted protein *KIAA0247*, the putative exonuclease *FLJ12484*, the recently identified *p53CSV* (*HSPC132*), and the serine-threonine kinase *CNK* (*PLK3*). The sequences of the putative p53REs in those genes are provided as Supplementary Table 3. Validation of the putative p53 target genes is currently under way in our laboratory.

Validation of array data by quantitative reverse transcription-PCR. For validation of the microarray results, we used quantitative real-time RT-PCR. We selected eight genes [*SNK* (*PLK2*), *PMAIP1, DDB2, CNK* (*PLK3*), *RAI3, POLE2, CPE*, and *CDKN1C*] with well-characterized functions related to, among

others, cell cycle, differentiation and division, DNA repair, apoptosis, and secretion. Overall, independent validation by RT-PCR showed a good correlation with the microarray analysis (Pearson $r = 0.822$, $P < 0.0001$). The data are presented as Supplementary Fig. 5 and Supplementary Tables 4 and 5. A more detailed description of the validation experiments is also available in the Supplement.

Discussion

The microenvironment of chronic inflammation can initiate carcinogenesis and drive tumor progression and metastasis (reviewed in ref. 2). The inflammatory microenvironment both activates the p53 network and inactivates the tumor suppressor activity by mutation of the *p53* gene (reviewed in refs. 2, 7, 21). We have selected four critical microenvironmental components, free radicals ($NO^{\bullet}$ and $OH^{\bullet}$), hypoxia, and DNA replication stress, and investigated their p53-dependent effects on gene expression. Global gene expression profiling of $TP53^{wt}$ and isogenic $TP53^{-/-}$ cells provides insight into a variety of cellular stress responses likely to occur under pathophysiologic conditions, such as ulcerative colitis (5, 22), that are associated with p53 activation.

Differentially regulated genes. Analysis of the time course–related genes (*F* test) revealed that the majority was down-regulated following cellular stress induced by $NO^{\bullet}$, H_2O_2, and hydroxyurea exposure. Similar down-regulation has been reported for H_2O_2 in other cell types (23, 24). Interestingly, the opposite was true for the cells under hypoxic conditions, which led to up-regulation of up to 80% of the genes in our study and others (25). Hypoxia-related induction of transcription factors like *HIF-1α* and *NF-κB* may contribute to the higher proportion of genes up-regulated by that exposure than by the others.

Analysis of p53-dependent gene expression profiles (*t* test) showed that 30% to 80% of genes modulated by $NO^{\bullet}$, H_2O_2, or hydroxyurea were repressed. In this regard, two recent microarray-based studies showed down-regulation of 50% of p53-responsive genes following cell cycle arrest and apoptosis in a *TP53*-transfected human lung carcinoma cell line (26) and a human ovarian cancer cell line (27). Although p53 is believed to function primarily as a sequence-specific transcriptional activator in the G_1 and G_2 phases of the cell cycle (28), it also mediates a variety of downstream functions by repressing target genes (29). In fact, it is estimated that up to 80% of p53-responsive genes are repressed rather than activated (30). Although p53 transactivator functions are far better understood, our understanding of p53 translational repression functions has improved in recent years. Three general mechanisms have been proposed (reviewed in ref. 31). First is the inhibition of recruitment of DNA-binding transcriptional activators, such as HNF-3, by competitive interference with p53. Second is the interference with the basal transcriptional machinery, as is the case for repression of *CYCLIN B2* by p53. We observed p53-mediated translational repression of *CYCLIN B2* only in cells exposed to $NO^{\bullet}$. Third is repression by p53 of target promoters through alterations of the chromatin structure (chromatin remodeling). With regard to the third mechanism, inhibition of histone deacetylases resulted in the loss of p53-dependent repression of *MAP4*, *β-TUBULIN*, and *SURVIVIN*. We previously showed p53-dependent down-regulation of *SURVIVIN* in human lymphoblastoid cells exposed to $NO^{\bullet}$ (3). These three mechanisms of p53 translational repression can also act in combination (32).

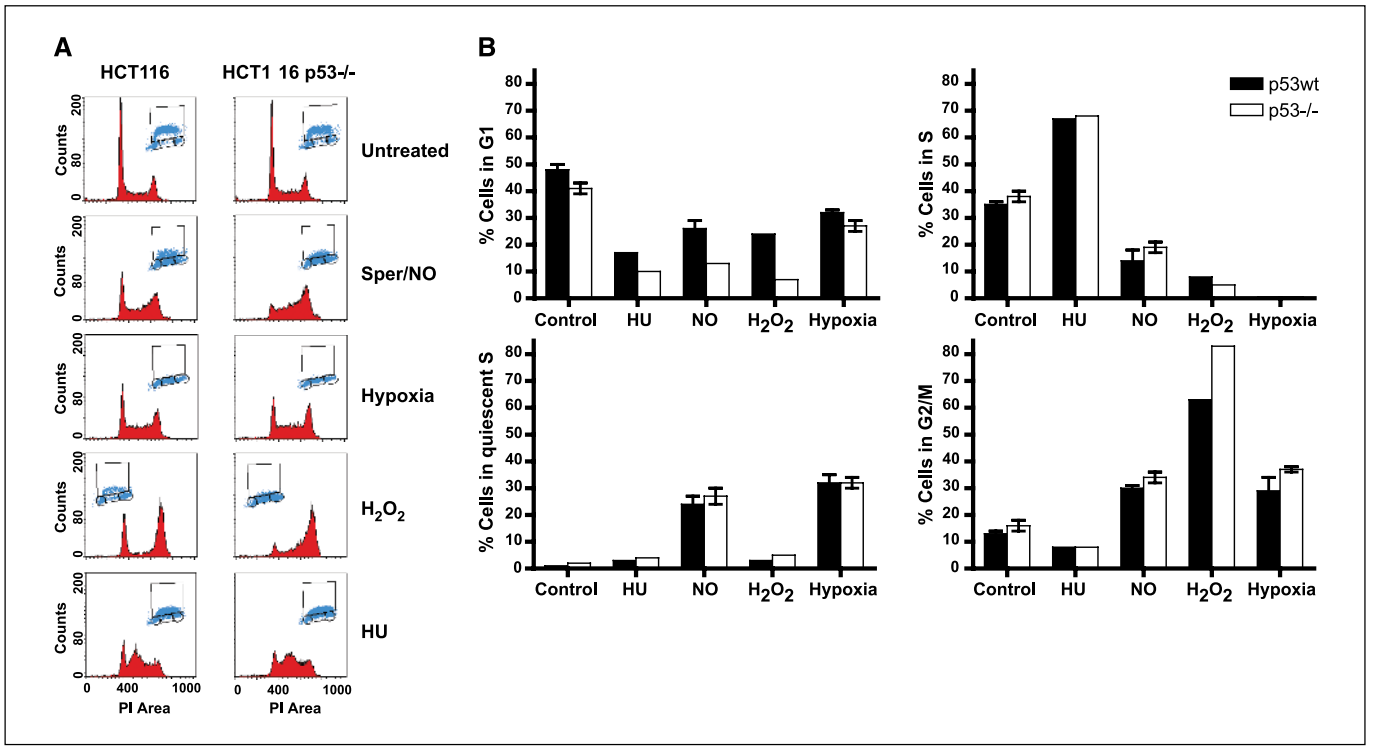

Figure 5. Functional cell cycle analysis by fluorescence-activated cell sorting. *A,* HCT116 and HCT116 $TP53^{-/-}$ cells were labeled with BrdUrd during the last 30 minutes of a 24-hour exposure as indicated, followed by double staining with FITC-conjugated anti-BrdUrd antibody and propidium iodide. *Insets,* gating used to calculate the fraction of cells in each phase of the cell cycle. *B, columns,* percentage of cells in each cell cycle phase of triplicate samples from one of two independent experiments; *bars,* SD. *Black columns,* HCT116 cells; *white columns,* HCT116 $TP53^{-/-}$ cells.

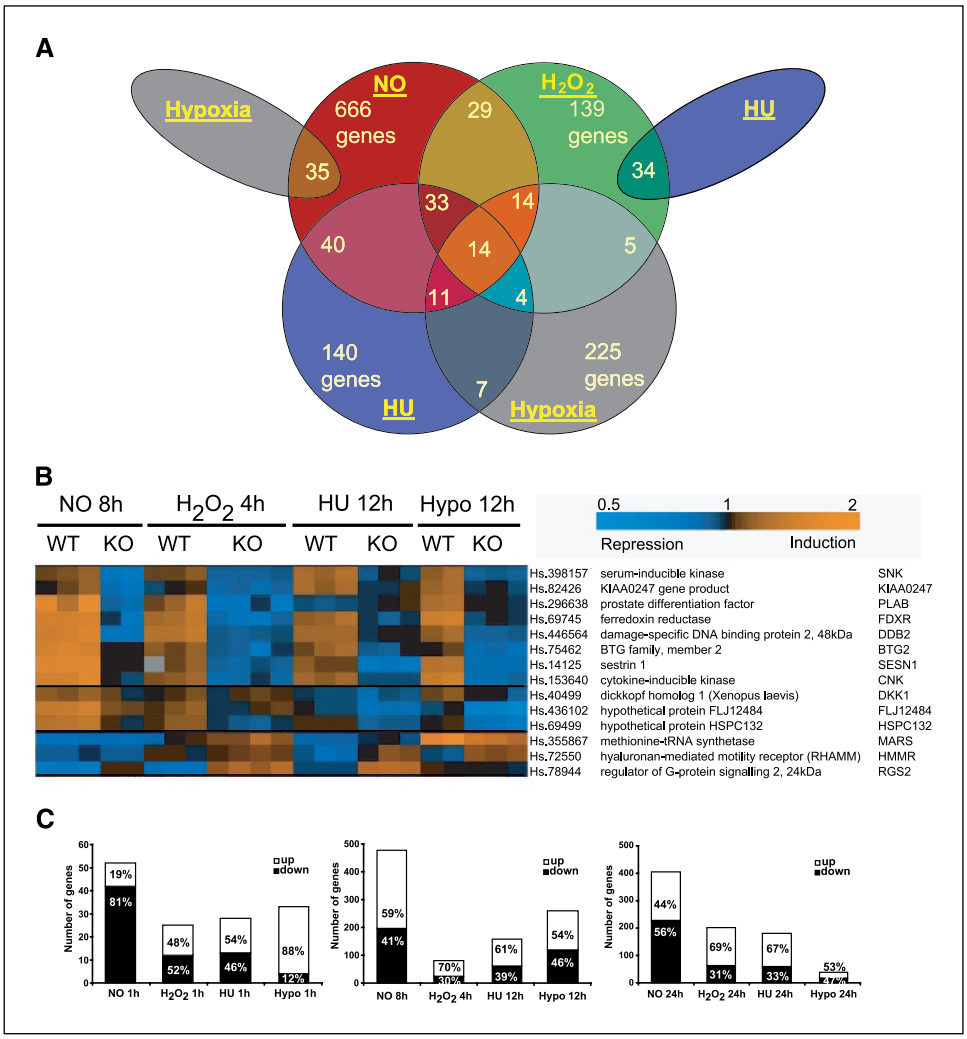

Figure 6. Analysis of p53-mediated stress-related genes as determined by the univariate *t* test with randomized variance model. *A,* Venn diagram based on the cumulative 1,396 genes that discriminate between $p53^{wt}$ and $p53^{-/-}$ cells at any time point in any treatment identified by paired comparison of the expression profile of $p53^{wt}$ and $p53^{-/-}$ cells at individual time points of exposure. There are 14 genes whose expression is dependent on the presence of p53 for all exposures. *B,* hierarchical clustering of the 14 overlapping genes. This cluster consists of the replicate arrays of the corresponding time points with maximal p53 accumulation for each treatment (Fig. 1). Color-coded degree of expression (0.5- to 2-fold) relative to the untreated samples (*top right*). *C,* total numbers of genes used to generate the Venn diagram are shown as ratio of up-regulated (*white columns*) and down-regulated (*black columns*). The genes are divided into 1-hour (*left*), intermediate (*middle*), and 24-hour (*right*) time points.

p53-dependent gene repression is also involved in negative feedback loops, including the *iNOS* (33) and the *CHEK2* (34) genes. Although the evidence for binding through p53RE as a mechanism for transcriptional repression is generally weak, p53 consensus DNA-binding sequences have been found among genes repressed in a p53-dependent manner (26, 27). We are currently searching for such p53REs in the upstream sequences of genes down-regulated in our microarray study.

We also found increased expression of 28 of 53 (53%) previously described up-regulated p53 target genes (Supplementary Table 1) among 746 genes up-regulated in a p53-mediated way as identified by *t* test. Included were *p21* (*CDKN1A*) and others associated with G_1 cell cycle arrest, as well as known apoptosis-related genes, such as *NOXA* and *BAX*. Those results are consistent with the role of p53 in the response to NO•-induced DNA damage (3).

One of the *TP53*-dependent genes, *WIG1*, was up-regulated by H_2O_2, hydroxyurea, and hypoxia. *WIG1* is a target for BMI1, recently found to be required for hematopoietic stem cell self-renewal (35). Like *WIG1*, BMI1 regulates additional survival and proliferation genes, such as $p19^{ARF}$ and $p16^{INK4A}$. Its expression is reported to be increased in colon cancers (36). Those observations provide a potential link of *TP53* function to stem cell renewal. The role of p53 in maintenance of normal and cancer stem cells is not known and warrants further investigation.

Hierarchical sample cluster analysis: similarities between NO• and hypoxia and hydroxyurea and H_2O_2. Interestingly, the gene expression profiles of cells exposed to NO• or hypoxia are similar to each other. So are those of cells exposed to H_2O_2 or hydroxyurea. Although HIF-1α accumulation is a hallmark of hypoxia, exposure to NO• can induce HIF-1α stabilization, DNA binding, and transactivation under normoxic conditions (reviewed in refs. 37, 38). HIF-1α and p53 are regulated by distinct threshold concentrations of NO• (39). HIF-1α is stabilized by lower concentrations of NO•, perhaps via inhibition of HIF-1α prolyl hydroxylation by attenuation of prolyl hydroxylase activity (reviewed in ref. 40). Higher concentrations of NO• are required for p53 accumulation via DNA strand breaks and activation of the ATM and ATR kinase networks (4). Opposing positive and negative feedback loops also exist. Hypoxia can cause an increase of *iNOS* expression (41–44), which, in turn, can lead to the induction of NO• and hypoxia-inducible genes (45). In a negative feed back loop, p53 translationally represses the transcription of *iNOS* (46). Those observations are consistent with our finding by hierarchical clustering of a similarity between gene expression changes under NO• exposure and those seen under hypoxic stress.

The gene expression profiles of cells exposed to hydroxyurea or H_2O_2 were also similar to each other, as shown by hierarchical sample clustering. Previous reports have suggested a link between

hydroxyurea- and H_2O_2-induced stresses. For example, the teratogenic and toxic effects of hydroxyurea are likely to be mediated by free radicals (47). Hydroxyurea may also induce site-specific DNA damage by the formation of H_2O_2 and NO• (48). Those prior observations suggest that hydroxyurea is likely to cause cellular and DNA damage by the formation of oxyradicals. The similarity of our gene expression profiles between hydroxyurea and H_2O_2 indirectly supports that hypothesis.

Functional validation of gene expression by cell cycle analysis. Consistent with the statistical analysis of gene expression, our cell cycle study also indicated similarities between the responses evoked by NO• and hypoxia exposures. Both exposures led to pronounced decrease in BrdUrd incorporation into cells with S-phase DNA content, a condition previously described as quiescent S phase (4, 15), as well as G_2-M arrest. Loss of BrdUrd incorporation was previously reported to occur within 30 minutes after exposure to NO• (4). Such a rapid decrease in BrdUrd incorporation suggests that NO• has a direct effect on DNA synthesis. NO• has been linked to depletion of the nucleotide pools (49) via a direct effect on enzymes such as the p53-dependent ribonucleotide reductase (RRM2B), which is involved in DNA repair and synthesis (reviewed in ref. 50). We found that *RRM2B* mRNA is decreased in *TP53*$^{-/-}$ cells following exposure to NO•. The shortage of deoxynucleotides, caused by direct and indirect effects on ribonucleotide reductases and other oxygen-dependent enzymes, such as dihydroorotate dehydrogenase, can also induce rapid S-phase arrest under hypoxia (51). Attenuated nucleotide pools can also limit DNA repair and increase genomic instability.

High-Throughput GoMiner analysis of *TP53*wt cells also revealed several cell cycle–related Gene Ontology categories similarly affected by NO• and hypoxia. The majority of the genes within these categories were down-regulated (Supplementary Fig. 6). Some individual genes in these categories overlapped between NO• and hypoxia. For example, among the genes significantly down-regulated by NO• and hypoxia within the Gene Ontology category "DNA replication," we identified DNA-directed polymerases and the BLM helicase (Supplementary Fig. 6*C*). This feature would be consistent with the appearance of a quiescent S phase. More often, the genes within a category were affected by only one exposure. This is more apparent when p53-dependent gene expression data is analyzed by High-Throughput GoMiner. NO• was the only stress condition with significantly affected genes belonging to the category "DNA replication" (and also cell cycle–related categories) in a p53-dependent manner (data not shown).

Inflammation generates a complex, intricate, highly coordinated stress response. Our study comprising only four components of inflammation, NO•, H_2O_2, DNA replication stress (i.e., by hydroxyurea exposure), and hypoxia, highlights that complexity. The p53 network is a major molecular participant in both the generic and particular patterns of gene expression, consistent with the known diversity in outcomes resulting from p53 activation in response to different stimuli by transactivating and translationally repressing target genes (1, 29). We found a few gene expression responses common to all four exposures, but a much larger number were idiosyncratic. Our observations also suggest that there is a common profile of early-response genes that are activated upon acute cellular stress, preceding a stress-specific response. Lastly, the pool of p53-dependent genes provides a resource for identifying potential novel biomarkers of the p53-dependent inflammatory response.

Acknowledgments

Received 5/20/2005; revised 8/5/2005; accepted 8/29/2005.

Grant support: Deutsche Forschungsgemeinschaft (F. Staib). This research was supported in part by the National Cancer Institute, Center for Cancer Research, and NIH Intramural Research Program.

The costs of publication of this article were defrayed in part by the payment of page charges. This article must therefore be hereby marked *advertisement* in accordance with 18 U.S.C. Section 1734 solely to indicate this fact.

We thank Dorothea Dudek for editorial assistance, Karen MacPherson for bibliographical assistance, and Kathleen Meyer and Esther Asaki for helping upload original microarray data into GEO.

References

1. Hofseth LJ, Hussain SP, Harris CC. p53: 25 years after its discovery. Trends Pharmacol Sci 2004;25:177–81.
2. Hussain SP, Hofseth LJ, Harris CC. Radical causes of cancer. Nat Rev Cancer 2003;3:276–85.
3. Li CQ, Robles AI, Hanigan CL, et al. Apoptotic signaling pathways induced by nitric oxide in human lymphoblastoid cells expressing wild-type or mutant p53. Cancer Res 2004;64:3022–9.
4. Hofseth LJ, Saito S, Hussain SP, et al. Nitric oxide-induced cellular stress and p53 activation in chronic inflammation. Proc Natl Acad Sci U S A 2003;100:143–8.
5. Hussain SP, Amstad P, Raja K, et al. Increased p53 mutation load in noncancerous colon tissue from ulcerative colitis: a cancer-prone chronic inflammatory disease. Cancer Res 2000;60:3333–7.
6. Hussain SP, Raja K, Amstad PA, et al. Increased p53 mutation load in nontumorous human liver of Wilson disease and hemochromatosis: oxyradical overload diseases. Proc Natl Acad Sci U S A 2000;97:12770–5.
7. Hofseth LJ, Hussain SP, Wogan GN, Harris CC. Nitric oxide in cancer and chemoprevention. Free Radic Biol Med 2003;34:955–68.
8. Ames BN, Gold LS, Willett WC. The causes and prevention of cancer. Proc Natl Acad Sci U S A 1995;92:5258–65.
9. Robles AI, Harris CC. p53-mediated apoptosis and genomic instability diseases. Acta Oncol 2001;40:696–701.
10. Sancar A, Lindsey-Boltz LA, Unsal-Kaccmaz K, Linn S. Molecular mechanisms of mammalian DNA repair and the DNA damage checkpoints. Annu Rev Biochem 2004;73:39–85.
11. Hammond EM, Green SL, Giaccia AJ. Comparison of hypoxia-induced replication arrest with hydroxyurea and aphidicolin-induced arrest. Mutat Res 2003;532:205–13.
12. Lewis JS, Lee JA, Underwood JC, Harris AL, Lewis CE. Macrophage responses to hypoxia: relevance to disease mechanisms. J Leukoc Biol 1999;6:889–900.
13. Hammond EM, Denko NC, Dorie MJ, Abraham RT, Giaccia AJ. Hypoxia links ATR and p53 through replication arrest. Mol Cell Biol 2002;2:1834–43.
14. Zhou J, Schmid T, Brune B. HIF-1α and p53 as targets of NO in affecting cell proliferation, death and adaptation. Curr Mol Med 2004;4:741–51.
15. Zolzer F, Stuben G, Knuhmann K, Streffer C, Sack H. Quiescent S-phase cells as indicators of extreme physiological conditions in human tumor xenografts. Int J Radiat Oncol Biol Phys 1999;45:1019–24.
16. Lawrence T, Bebien M, Liu GY, Nizet V, Karin M. IKKα limits macrophage NF-κB activation and contributes to the resolution of inflammation. Nature 2005;434:1138–43.
17. Imhof A, Heinzer I. Continuous monitoring of oxygen concentrations in several systems for cultivation of anaerobic bacteria. J Clin Microbiol 1996;34:1646–8.
18. Zeeberg BR, Qin H, Narasimhan S, et al. High-Throughput GoMiner, an "industrial-strength" integrative Gene Ontology tool for interpretation of multiple-microarray experiments, with application to studies of Common Variable Immune Deficiency (CVID). BMC Bioinformatics 2005;6:168.
19. Bard J. Ontologies: formalising biological knowledge for bioinformatics. Bioessays 2003;25:501–6.
20. Stormo GD, Hartzell GW III. Identifying protein-binding sites from unaligned DNA fragments. Proc Natl Acad Sci U S A 1989;86:1183–7.
21. Coussens LM, Werb Z. Inflammation and cancer. Nature 2002;420:860–7.
22. Hofseth LJ, Khan MA, Ambrose M, et al. The adaptive imbalance in base excision-repair enzymes generates microsatellite instability in chronic inflammation. J Clin Invest 2003;12:1887–94.
23. Weigel AL, Handa JT, Hjelmeland LM. Microarray analysis of H2O2-, HNE-, or tBH-treated ARPE-19 cells. Free Radic Biol Med 2002;3:1419–32.
24. Chuang YY, Chen Y, Gadisetti, et al. Gene expression after treatment with hydrogen peroxide, menadione, or *t*-butyl hydroperoxide in breast cancer cells. Cancer Res 2002;62:6246–54.
25. Denko NC, Fontana LA, Hudson KM, et al. Investigating hypoxic tumor physiology through gene expression patterns. Oncogene 2003;2:5907–14.
26. Robinson M, Jiang P, Cui J, et al. Global genechip profiling to identify genes responsive to p53-induced growth arrest and apoptosis in human lung carcinoma cells. Cancer Biol Ther 2003;2:406–15.
27. Mirza A, Wu Q, Wang L, et al. Global transcriptional program of p53 target genes during the process of

apoptosis and cell cycle progression. Oncogene 2003;2: 3645–54.
28. Vogelstein B, Lane D, Levine AJ. Surfing the p53 network. Nature 2000;408:307–10.
29. Zhao R, Gish K, Murphy M, et al. Analysis of p53-regulated gene expression patterns using oligonucleotide arrays. Genes Dev 2000;14:981–93.
30. Wang L, Wu Q, Qiu P, et al. Analyses of p53 target genes in the human genome by bioinformatic and microarray approaches. J Biol Chem 2001;276: 43604–10.
31. Ho J, Benchimol S. Transcriptional repression mediated by the p53 tumour suppressor. Cell Death Differ 2003;10:404–8.
32. Sengupta S, Shimamoto A, Koshiji M, et al. Tumor suppressor p53 represses transcription of RECQ4 helicase. Oncogene 2005;24:1738–48.
33. Forrester K, Ambs S, Lupold SE, et al. Nitric oxide-induced p53 accumulation and regulation of inducible nitric oxide synthase (NOS2) expression by wild-type p53. Proc Natl Acad Sci U S A 1996;93: 2442–7.
34. Matsui T, Katsuno Y, Inoue T, et al. Negative regulation of Chk2 expression by p53 is dependent on the CCAAT-binding transcription factor NF-Y. J Biol Chem 2004;279:25093–100.
35. Park IK, Qian D, Kiel M, et al. Bmi-1 is required for maintenance of adult self-renewing haematopoietic stem cells. Nature 2003;423:302–5.
36. Kim JH, Yoon SY, Kim CN, et al. The Bmi-1 oncoprotein is overexpressed in human colorectal cancer and correlates with the reduced p16INK4a/p14ARF proteins. Cancer Lett 2004;203:217–24.
37. Brune B, Zhou J. The role of nitric oxide (NO) in stability regulation of hypoxia inducible factor-1α (HIF-1α). Curr Med Chem 2003;10:845–55.
38. Kasuno K, Takabuchi S, Fukuda K, et al. Nitric oxide induces hypoxia-inducible factor 1 activation that is dependent on MAPK and phosphatidylinositol 3-kinase signaling. J Biol Chem 2004;279:2550–8.
39. Thomas DD, Espey MG, Ridnour LA, et al. Hypoxic inducible factor 1α, extracellular signal-regulated kinase, and p53 are regulated by distinct threshold concentrations of nitric oxide. Proc Natl Acad Sci U S A 2004;101:894–9.
40. Zhou J, Brune B. NO and transcriptional regulation: from signaling to death. Toxicology 2005;208: 223–33.
41. Jung F, Palmer LA, Zhou N, Johns RA. Hypoxic regulation of inducible nitric oxide synthase via hypoxia inducible factor-1 in cardiac myocytes. Circ Res 2000;86:319–25.
42. Park SY, Lee H, Hur J, et al. Hypoxia induces nitric oxide production in mouse microglia via p38 mitogen-activated protein kinase pathway. Brain Res Mol Brain Res 2002;107:9–16.
43. Palmer LA, Semenza GL, Stoler MH, Johns RA. Hypoxia induces type II NOS gene expression in pulmonary artery endothelial cells via HIF-1. Am J Physiol 1998;274:L212–9.
44. Melillo G, Musso T, Sica A, Taylor LS, Cox GW, Varesio L. A hypoxia-responsive element mediates a novel pathway of activation of the inducible nitric oxide synthase promoter. J Exp Med 1995;182:1683–93.
45. Chun YS, Kim MS, Park JW. Oxygen-dependent and -independent regulation of HIF-1α. J Korean Med Sci 2002;17:581–8.
46. Ambs S, Ogunfusika MO, Merriam WG, Bennett WP, Billiar TR, Harris CC. Upregulation of NOS2 expression in cancer-prone p53 knockout mice. Proc Natl Acad Sci U S A 1998;95:8823–8.
47. DeSesso JM. Cell death and free radicals: a mechanism for hydroxyurea teratogenesis. Med Hypotheses 1979;5:937–51.
48. Sakano K, Oikawa S, Hasegawa K, Kawanishi S. Hydroxyurea induces site-specific DNA damage via formation of hydrogen peroxide and nitric oxide. Jpn J Cancer Res 2001;92:1166–74.
49. Fontecave M. Ribonucleotide reductases and radical reactions. Cell Mol Life Sci 1998;54:684–95.
50. Roy B, Guittet O, Beuneu C, Lemaire G, Lepoivre M. Depletion of deoxyribonucleoside triphosphate pools in tumor cells by nitric oxide. Free Radic Biol Med 2004;36:507–16.
51. Green SL, Giaccia AJ. Tumor hypoxia and the cell cycle: implications for malignant progression and response to therapy. Cancer J Sci Am 1998;4:218–23.